

GHGT-10

Reducing the risk of well bore leakage of CO₂ using engineered biomineralization barriers

A. B. Cunningham¹, R. Gerlach¹, L. Spangler², A.C. Mitchell^{1,3}, S. Parks¹, and A. Phillips¹

¹Center for Biofilm Engineering, Montana State University, Bozeman, MT, USA.

²Department of Chemistry and Biochemistry, Montana State University, Bozeman, MT, USA.

³Institute of Geography and Earth Sciences, Aberystwyth University, UK.

Abstract

If CO₂ is injected in deep geological formations it is important that the receiving formation has sufficient porosity and permeability for storage and transmission and be overlain by a suitable low-permeability cap rock formation. When the resulting CO₂ plume encounters a well bore, leakage may occur through various pathways in the “disturbed zone” surrounding the well casing. Gasda et al.[9], propose a method for determining effective well bore permeability from a field pressure test. If permeability results from such tests prove unacceptably large, strategies for *in situ* mitigation of potential leakage pathways become important. To be effective, leakage mitigation methods must block leakage pathways on timescales longer than the plume will be mobile, be able to be delivered without causing well screen plugging, and be resistant to supercritical CO₂ (ScCO₂) challenges. Traditional mitigation uses cement, a viscous fluid that requires a large enough aperture for delivery and that also must bond to the surrounding surfaces in order to be effective. Technologies that can be delivered via low viscosity fluids and that can effectively plug small aperture pathways, or even the porous rock surrounding the well could have significant advantages for some leakage scenarios.

We propose a microbially mediated method for plugging preferential leakage pathways and / or porous media, thereby lowering the risk of unwanted upward migration of CO₂, similar to that discussed by Mitchell et al.[12]. We examine the concept of using engineered microbial biofilms which are capable of precipitating crystalline calcium carbonate using the process of ureolysis. The resulting combination of biofilm plus mineral deposits, if targeted near points of CO₂ injection, may result in the long-term sealing of preferential leakage pathways. Successful development of these biologically-based concepts could result in a CO₂ leakage mitigation technology which can be applied either before CO₂ injection or as a remedial measure. Results from laboratory column studies are presented which illustrate how biomineralization deposits can be developed along packed sand columns at length scales of 2.54 cm and 61 cm. Strategies for controlling mineral deposition of uniform thickness along the axis of flow are also discussed.

© 2011 Published by Elsevier Ltd. Open access under [CC BY-NC-ND license](https://creativecommons.org/licenses/by-nc-nd/4.0/).

Keywords: Biofilm; Biomineralization; Calcium Carbonate; Supercritical CO₂; Well Bore Integrity

1.0 Introduction

Geologic carbon sequestration involves the injection of CO₂ into underground formations including oil beds, deep un-minable coal seams, and deep saline aquifers with temperature and pressure conditions such that CO₂ will likely be in the supercritical state (ScCO₂). The upward movement of the ScCO₂ plume will be limited by the low-permeability cap rock that would typically bound the aquifer above. However, if preferential flow pathways exist through the cap rock unwanted upward migration of CO₂ into shallower zones will very likely occur as shown conceptually in Figure 1. A concept for reducing the risk of well bore leakage (i.e. leakage mitigation) of CO₂ based on the use of engineered microbial biofilms which are capable of biomineralization has been proposed by Cunningham et al.[2] and Mitchell et al.[11, 12].

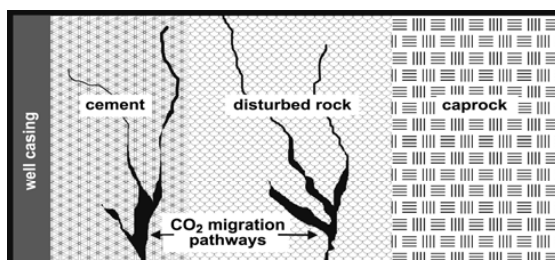


Figure 1. Schematic showing potential CO₂ leakage pathways in disturbed rock, cement and along well casing. This schematic represents the cement layer and disturbed rock at a location where the well passes through the cap rock, above the reservoir.

The engineered biomineralization process produces biofilm and mineral deposits that reduce the permeability of geologic media while modifying the geochemistry of brines to enhance CO₂ solubility and mineral precipitation [11]. These processes can be targeted in the vicinity of geologic sequestration injection wells to provide long-term sealing of preferential leakage pathways. Because the fluids used to initiate biofilm formation and biomineralization are low viscosity aqueous solutions, this technology has the potential to seal small aperture leaks or the porous rock itself potentially providing a leakage mitigation technique that can address issues problematic for cement use.

2.0 Biomineralization by Ureolysis

Carbonate mineral formation in the subsurface can be engineered through the bacterial hydrolysis of urea (ureolysis). Ureolysis can occur under dark subsurface conditions and results in the production of ammonium (NH₄⁺), an increase in pH, an increase in alkalinity (Eqs. 1-5), and ultimately oversaturation of the aqueous phase with respect to carbonate minerals, such as CaCO₃ (Eq. 6) [5, 6, 11, 14]. Carbonate mineral formation can be engineered by controlling the concentration and activity of microorganism, the supply of Ca²⁺ and HCO₃⁻, growth nutrients, or urea availability. Urease (the enzyme responsible for urea hydrolysis) is common in a wide variety of microorganisms [17] and can therefore be readily and inexpensively induced by adding urea. Consequently microbial ureolysis has been investigated for industrial utilities such as mineral plugging [6, 7] and immobilizing calcium and contaminants in surface and groundwater [3, 10, 14].





3.0 Research Approach

The challenge at hand is to engineer the biomineralization process to be effective in the subsurface environment near the wellbore (Figure 1). Before this technology can be considered operational it must be demonstrated that (1) mineral deposits can be formed at a field relevant scale under environmental conditions appropriate to subsurface reservoirs, (2) the mineral deposition can be kept uniform over relevant distances, (3) the degree of sealing in disturbed rock, cement, and cement-well bore interfaces reaches an acceptable level, and (4) the biomineral deposits are stable when exposed to brine and ScCO_2 . Prior to demonstrating this technology in the field it is essential to first conduct proof-of-principal experiments aimed at addressing each of these scale-up issues. The bench-scale column results reported here advance this risk-reduction strategy by demonstrating the ability to control the deposition of mineral (i.e. calcium carbonate) uniformly along the porous media flow path.

4.0 Injection Strategy to Control the Spatial Distribution of a Biomineralized Barrier

In previous studies [2, 16, 18] high amounts of calcium carbonate were observed near injection sites that decreased over the length of the flow path, leading to a restricted transport of nutrients. In fact in previous two-dimensional reactor flow experiments, after approximately 20 hours of operation the capacity of the pump was exceeded (and flow through the reactor ceased) as the reactor had become completely plugged with calcium carbonate crystals [2, 16]. In order to effectively seal larger areas of preferential leakage pathways in a field application with biomineralized barriers, the precipitation reaction must extend radially outward from the well bore. Effectiveness of a field scale delivery also requires new field-scale monitoring techniques [8] to test parameters such as concentrations, flow rates, abundance and activity of microorganisms to determine spatial distribution of biomineralized barriers [16]. Other researchers [18] hypothesize that in order to produce a more homogenous precipitation along the flow path, the balance between nutrient and calcium supply and conversion to mineral needs to be shifted by controlling injection flow rates.

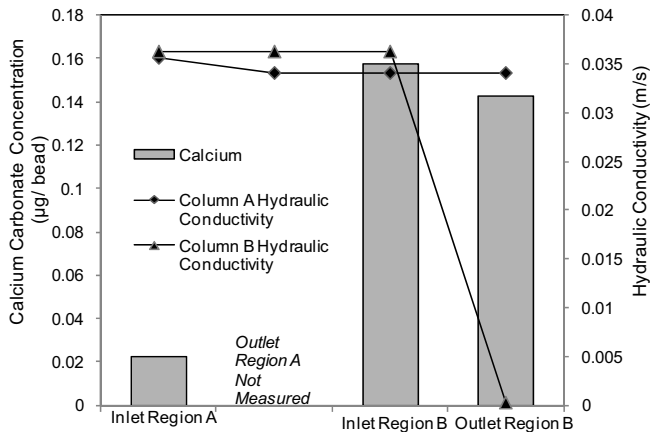


Figure 2. Distribution of Calcium Carbonate Deposits and Hydraulic Conductivity in 1 cm diameter, 2.5 cm long columns packed with 1 mm glass beads. Column A was injected with media containing 0.025 M Ca^{2+} and Column B with media containing 1.25M Ca^{2+} over 17 days. Plugging and homogenous calcium distribution (between inlet and outlet) was achieved in Column B. Plugging was not achieved in Column A.

Previously unpublished studies performed in our lab in 2.5 cm glass bead-packed columns inoculated with a known ureolytic bacterium, *Sporosarcina pasteurii* (formerly *Bacillus pasteurii*), showed column plugging and homogenous calcium carbonate precipitation could be achieved over short distances by controlling calcium concentrations in the growth medium (Figure 2). Two columns were run, with two different calcium concentrations of 1.25 M and 0.025 M in order to assess the effect on the spatial distribution of calcium carbonate precipitation. Lower calcium concentrations did not result in significant reductions in hydraulic conductivity over the course of the experiment, whereas higher concentrations resulted in complete plugging and homogenous distribution of calcium between inlet and outlet regions.

5.0 Methods for Investigating Biomineralization in Sand-Packed Columns

Based on results from the 2.5 cm columns, the ability of urea hydrolyzing (ureolytic) biofilms to stimulate CaCO_3 mineral formation was subsequently investigated in a vertically positioned 61 cm long, 2.54 cm diameter column packed with 40 mesh (0.5 mm effective size in filtration) quartz sand (Unimin Corporation, Emmet, ID). The column was inoculated with *Sporosarcina pasteurii* and growth medium was added over 18 hours to develop a biofilm. After biofilm establishment, a calcium-rich (1.25 M calcium) growth medium was injected into the column to initiate biomineralization. The columns were filled with two pore volumes of calcium-rich medium and allowed to remain static for 24 hours (biomineralization stage). Between biomineralization stages, the column was flushed with two pore volumes of calcium-free media prior to re-injecting another two pore volumes of fresh calcium-rich medium. This filling/flushing injection strategy occurred 36 times in a 58 day period. On five different periodic occasions throughout the 58 day experiment, the biofilm was refreshed by flowing at least two pore volumes of fresh growth medium without calcium. During injection, flushing or refreshing, growth or calcium-rich medium was flowed at 10 ml/min and controlled by a Masterflex (Model 7553-70) pump and controller (Cole Parmer, Vernon Hills, IL).

The growth and calcium-rich growth media were produced by mixing three grams of Difco Nutrient Broth (BD, Sparks, MD), 20 grams of urea (Fisher, Fair Lawn, NJ), 10 grams of ammonium chloride (Fisher, Fair Lawn, NJ), and 185 grams of calcium chloride dihydrate (not included in growth medium without calcium) (Acros, NJ, USA) and stirring continuously until dissolved in 1 L of nanopure water. As necessary, the pH of the media was adjusted to between 6.0 and 6.3. Complete medium was filter sterilized using a SteriTop (Fisher, Fair Lawn, NJ) 0.22 μm vacuum filter.

Throughout the experiment ammonium production, residual effluent dissolved calcium concentration, pressure drop (hydraulic head) across the column, and effective porosity were monitored. To measure effluent ureolysis activity and dissolved calcium, the column effluent was collected after each 24 hour biomineralization batch period. A portion of the effluent sample was filtered using a 0.2 μm SFCA Corning syringe filter (Corning Incorporated, NY) and analyzed with a modified Nessler Assay for ammonium production (direct product of ureolysis), and Inductively Coupled Plasma Mass Spectrometry (ICP-MS) for dissolved calcium concentration. The unfiltered remainder of the effluent sample was used to monitor pH. Hydraulic head was measured using water-filled piezometers and effective porosity was measured by residence time distribution analysis (tracer studies) using fluorescein dye tracer.

Details of the methods used to monitor column activity were as follows: Ammonium was determined with a modified Nessler method: Effluent samples were diluted in deionized water and compared to standards made from $(\text{NH}_4)_2\text{SO}_4$. Each sample and standard (250 μL) was added in triplicate to a 96-well microplate (Fisher, Fair Lawn NJ), to which 3 μL of mineral stabilizer and polyvinyl alcohol, and 10 μL of Nessler reagent (potassium tetraiodomercurate(II)) (Hach,

Loveland, CO), were added. Concentration of ammonium was quantified in the resulting solution after 13 minutes reaction time via spectrophotometry at 425 nm (BioTek, Synergy HT). The pH of effluent samples was assessed with a Fisher Scientific pH meter (model 50) equipped with a Corning glass electrode, which was calibrated daily with pH 7 and 10 buffers. Concentrations of dissolved (0.20 μm filtered) calcium were measured on an Agilent 7500 ICP-MS after a 1:5000 dilution in 5 % Trace Metal Grade Nitric Acid (Fisher, Fair Lawn, NJ) and compared with certified standards (Agilent Technologies, Environmental Calibration Standard 5183-4688). The differential pressure between influent and effluent water-filled piezometers was measured to determine changes in hydraulic head. During tracer studies 1 mL of a 1 g/L solution of fluorescein dye was injected at the column influent and 200 μL effluent samples were taken at regular time intervals and transferred to a 96-well plate. Fluorescence was measured at 485/528 nm excitation/emission (Biotek, Synergy HT). The peak of the curve of fluorescence was found and compared to the volume of effluent flowed during the study to find effective porosity [16].

At the termination of the experiment, the column was destructively sampled by cutting it into eight 7.6 cm sections and digesting a portion of each section's sand contents with 10% Trace Metal Grade Nitric Acid (Fisher, Fair Lawn, NJ) for analysis with ICP-MS to determine total calcium carbonate mineral per mass of sand. This was performed in triplicate for each section. Additionally, stereoscope images of the biofilm-mineral deposits were taken.

6.0 Results and Discussion

Effect of Biomineralization on Residual Effluent Solution

Urea hydrolysis was apparent during the duration of the experiment from the production of ammonium and an increase in pH in the effluent of the column (data not shown). Effluent ammonium concentration decreased in the final 15 days of the experiment indicating possibly decreased ureolytic activity. Ammonium concentration in the effluent may have dropped due to calcium carbonate precipitation being a highly lethal event for *S. pasteurii* [4] or bacterial activity declining over time due to a cementation diffusion barrier surrounding the cells [18]. Some bacteria may act as nucleation points for CaCO_3 crystal formation, and become encased in mineral creating diffusion barriers [1, 15].

CaCO_3 Profile and Occupied Pore Space along Length of the Column

After 58 days, biofilm-mineral deposits resulted in complete plugging of the column (i.e. growth media could no longer be pumped through the column). The average calcium carbonate content, measured as mg CaCO_3 per gram of sand was 479 ± 29 mg CaCO_3/g sand in the first section near the inlet of the column (Figure 3). The mass was lower for the remaining five sections in the column, averaging 239 ± 26 mg/g (Figure 3). This somewhat constant mass distribution of calcium carbonate is encouraging for achieving uniform calcium carbonate distribution along the flow path, particularly when compared with similar results from other studies [1, 18]. However, the 490 mg CaCO_3/g sand value near the column entrance is still considered unacceptably high. Strategies for reducing deposition near the entrance are discussed in section 8.0 below.

Multiplying the analytically determined mass of calcium carbonate by an assumed CaCO_3 density of 2.7 g/cm^3 and an assuming an initial porous media porosity of 40%, the volume fraction of pore space occupied by precipitated calcium carbonate was calculated (Figure 3). Calcium carbonate was calculated to occupy 28.2% of the pore space in the first 7.6 cm section of the column and between 11 and 16% in the remainder of the column, with an overall average of $15.8\% \pm 5.2\%$ over the length of the column.

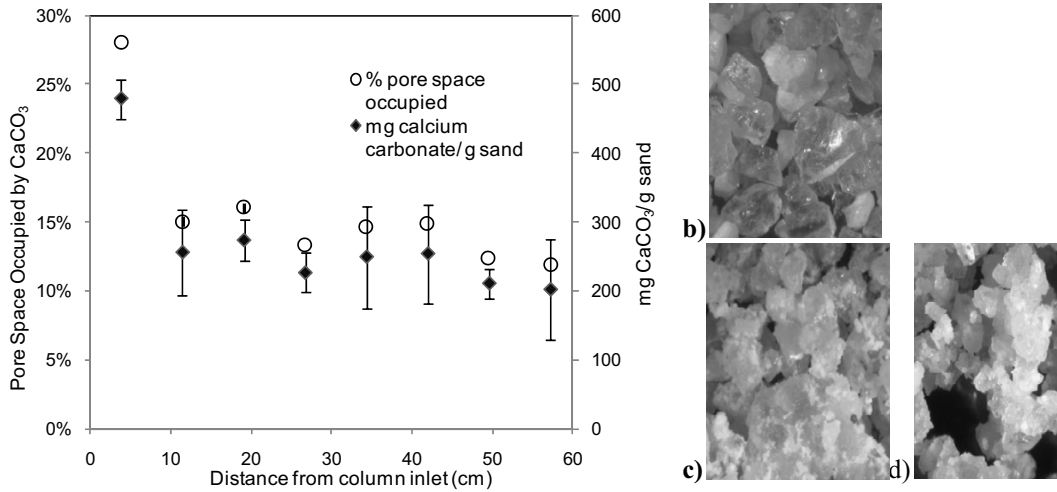


Figure 3. (a) Volume fraction of calcium carbonate-occupied pore space and CaCO₃ concentrations over the distance of the column. Stereoscopic analysis of (b) clean sand (control) and biofilm-calcium carbonate deposits (c - first 7.6 cm of column) and (d - last 7.6 cm of column) reveal significant calcium carbonate deposits.

Effect of Precipitation on Pore Space Properties

Figure 4 shows the reduction in hydraulic conductivity along with the volume fraction of pore space occupied by CaCO₃ for the entire column as measured by tracer analysis. Tracer studies were used to measure effective porosity which was converted to an occupied pore space volume fraction.

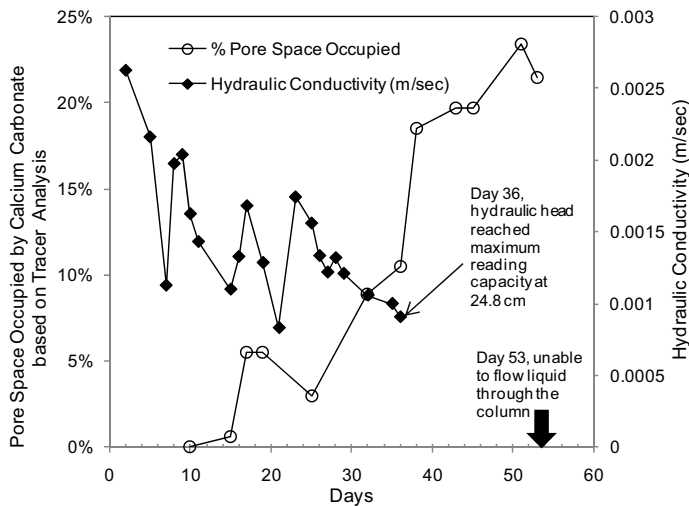


Figure 4. Relative decrease in pore space over time in the column (based on tracer analysis) and decrease in hydraulic conductivity observed over the first 36 days of the column experiment.

A 66% reduction in hydraulic conductivity was observed in the 61 cm column over the first 36 days (2.63×10^{-3} m/sec on day 2; 9.1×10^{-4} m/sec on day 36), at which point the limit of detection for the piezometer system was reached and no further hydraulic conductivity measurements were taken. Tracer analysis of effective porosity shows that 21.6 % of the pore space was occupied by CaCO₃ at

the conclusion of the experiment (initial pore space 162 cm^3 , final pore space 127 cm^3). This value can be compared with the average % pore space occupied by CaCO_3 measured in Figure 3, which was found to be $15.8 \% \pm 5.2 \%$. These values, as measured by two different methods, agree favorably and confirm extensive mineral precipitate occupying the pore space of the column. Previous research reported a 10% decrease in porosity in a 5 meter column calcium carbonate soil strengthening experiment [18].

7.0 Summary

The results reported herein demonstrate that:

- 1) The amount of CaCO_3 deposition (measured as $\text{mg CaCO}_3/\text{g sand}$) resulting from ureolytic biomineralization in flowing sand columns can be controlled by varying the concentration of Ca^{2+} in the nutrient feed. Calcium concentrations of 1.25 M resulted in extensive reduction in media hydraulic conductivity (i.e. capacity of pump was exceeded).
- 2) By varying the addition of calcium in the nutrient feed with a filling/flushing injection strategy with a Ca-inclusive then Ca-free media, a quasi-uniform CaCO_3 distribution was achieved along the 61 cm column with the exception of the first 7.6 cm section.

These results suggest that biofilm and biomineralization deposits may be engineered so as to reduce porosity and hydraulic conductivity of porous media. Successful development of these biologically-based technologies will result in CO_2 leakage mitigation strategies which can be applied either before CO_2 injection or as a remedial measure.

8.0 Current and Future Work

Further injection strategies to produce more homogenous biofilm-mineral plugging are being investigated, particularly to avoid the higher concentration of CaCO_3 near the column inlet. It is hypothesized that flushing the column entrance with calcium-free media after the calcium-rich media pulse will reduce influent point plugging and contribute to a more uniform precipitation distribution. Additionally, we are currently examining the effect of initial microorganism distribution, biofilm development in porous media, and changing flow rates of injection to achieve the homogenous distribution goal. These studies will promote understanding of injection strategies to deploy a successful field scale biomineralization barrier leakage mitigation technology.

9.0 Acknowledgements

Funding for this research was provided by the Zero Emissions Research and Technology (ZERT) program (DOE Award No. DE-FC26-04NT42262) and the US Department of Energy EPSCoR program under grant number DE-FG02-08ER46527. DOE EPSCoR funding was used to complete biomineralization studies using 2.54 cm columns while ZERT funding supported the 61 cm column work. Any opinions, conclusions, findings or recommendations expressed herein are those of the authors and do not necessarily reflect those of DOE. Also, the authors acknowledge funding for the establishment and operation of the Environmental and Biofilm Mass Spectrometry Facility at Montana State University (MSU) through the Defense University Research Instrumentation Program (DURIP, Contract Number: W911NF0510255) and the MSU Thermal Biology Institute from the NASA Exobiology Program (Project NAG5-8807).

10.0 References cited

1. Achal, V., Mukherjee, A., Basu, P.C, and Reddy, M.S. Lactose mother liquor as an alternative nutrient source for microbial concrete production by *Sporosarcina pasteurii*. *Journal Ind. Microbiol. Biotechnol.* 36: (2009) 433-438.
2. Cunningham, A.B., R. Gerlach, L. Spangler, A.C. Mitchell. (2009): Microbially enhanced geologic containment of sequestered supercritical CO₂. *Energy Procedia* 1(1):3245-3252.
3. Curti E. Coprecipitation of radionuclides with calcite: estimation of partition coefficients based on a review of laboratory investigations and geochemical data. *Applied Geochemistry* 14(4), (1999) 433-445.
4. Dupraz, S., Ménéz, B., Gouze, P., Leprovost, R., Bénézech, P., Pokrovsky, O.S., Guyot, F. Experimental approach of CO₂ biomineralization in deep saline aquifers. *Chemical Geology* 265: (2009) 54-62.
5. Ferris FG, Phoenix V, Fujita Y, Smith RW. Kinetics of calcite precipitation induced by ureolytic bacteria at 10 to 20 degrees C in artificial groundwater. *Geochimica Et Cosmochimica Acta* 68: (2003)1701-1710.
6. Ferris FG, Stehmeier LG, Kantzas A, Mourits FM. Bacteriogenic mineral plugging. *Journal of Canadian Petroleum Technology* 35: (1996) 56-61.
7. Ferris FG, Stehmeier LG. 1992. Bacteriogenic mineral plugging. United States Patent 6401819
8. Fujita, Y., Taylor, J.L., Gresham, T.L.T, Delwiche, M.E., Colwell, F.S., Mcling, T.L., Petzke, L.M., and Smith, R.W. Stimulation of Microbial Urea Hydrolysis in Groundwater to Enhance Calcite Precipitation. *Environmental Science and Technology* 42: (2008) 3025-3032.
9. Gasda S.E., J.M. Nordbotten, and M.A. Celia. Determining effective wellbore permeability from a field pressure test: a numerical analysis of detection limits. *Environ Geol* 54: (2008) 1207-1215.
10. Hammes F, Seka A, Van Hege K, Van de Wiele T, Vanderdeelen J, Siciliano SD, Verstraete W. Calcium removal from industrial wastewater by bio-catalytic CaCO₃ precipitation. *Journal of Chemical Technology and Biotechnology* 78: (2003) 670-677.
11. Mitchell A.C., K. Dideriksen, L.H. Spangler, A. B. Cunningham, R. Gerlach. Microbially enhanced carbon capture and storage by mineral-trapping and solubility-trapping. *Environmental Science and Technology* 44(13): (2010) 5270-5276.
12. Mitchell, A.C., A. Phillips, R. Hiebert, R. Gerlach, and A.B. Cunningham. Biofilm enhanced subsurface sequestration of supercritical CO₂. *International Journal Greenhouse Gas Control* Vol 3(1): (2009) 90-99.
13. Mitchell, AC and Ferris, FG. The influence of *Bacillus pasteurii* on the nucleation and growth of Calcium Carbonate. *Geomicrobiology Journal* 23: (2006) 213-226.
14. Mitchell, AC. and F.G. Ferris. The Co-Precipitation of Sr into Calcite Precipitates Induced by Bacterial Ureolysis in Artificial Groundwater – Temperature and Kinetic Dependence. *Geochimica Et Cosmochimica Acta* 69: (2005) 4199-4210.
15. Parks, S.L. Kinetics of Calcite Precipitation by Ureolytic Bacteria under Aerobic and Anaerobic Conditions. MS Thesis. March 2009, Montana State University, Bozeman MT.
16. Schultz, L. Reactive Transport in Biofouled and Biomineralized Porous Media. MS Thesis. January 2010, Montana State University, Bozeman MT.
17. Swensen B. and Bakken L. R. Nitrification potential and urease activity in a mineral subsoil. *Soil Biology & Biochemistry* 30(10-11): (1998) 1333-1341.
18. Whiffin, V.S., van Paassen, L.A., and Harkes, M.P. Microbial Carbonate Precipitation as a Soil Improvement Technique. *Geomicrobiology Journal* 24: (2007) 1-7.